

# A sample of radio-loud QSOs at redshift $\sim 4$

J. Holt,<sup>1,4\*</sup> C. R. Benn,<sup>1</sup> M. Vigotti,<sup>2</sup> M. Pedani,<sup>3</sup> R. Carballo,<sup>5</sup>  
J. I. González-Serrano,<sup>6</sup> K.-H. Mack<sup>2,7,8</sup> and B. García<sup>1</sup>

<sup>1</sup>Isaac Newton Group, Apartado 321, E-38700 Santa Cruz de La Palma, Spain

<sup>2</sup>Istituto di Radioastronomia, CNR, via Gobetti 101, I-40129 Bologna, Italy

<sup>3</sup>Centro Galileo Galilei, E-38700 Santa Cruz de La Palma, Spain

<sup>4</sup>Department of Physics & Astronomy, University of Sheffield, Hicks Building, Sheffield S3 7RH

<sup>5</sup>Departamento de Matemática Aplicada y C. Computació, Universidad de Cantabria, E-39005 Santander, Spain

<sup>6</sup>Instituto de Física de Cantabria (CSIC-UC), Facultad de Ciencias, E-39005 Santander, Spain

<sup>7</sup>ASTRON/NFRA, Postbus 2, NL-7990 AA Dwingeloo, the Netherlands

<sup>8</sup>Radioastronomisches Institut der Universität Bonn, Auf dem Hügel 71, D-53121 Bonn, Germany

Accepted 2003 November 5. Received 2003 November 5; in original form 2003 June 4

## ABSTRACT

We obtained spectra of 60 red, star-like objects ( $E < 18.8$ ) identified with FIRST radio sources,  $S_{1.4\text{GHz}} > 1$  mJy. Eight are quasi-stellar objects (QSOs) with redshift  $z > 3.6$ . Combined with our earlier pilot search, our sample of 121 candidates yields a total of 18  $z > 3.6$  QSOs (10 of these with  $z > 4.0$ ). 8 per cent of candidates with  $S_{1.4\text{GHz}} < 10$  mJy and 37 per cent of candidates with  $S_{1.4\text{GHz}} > 10$  mJy are QSOs with  $z > 3.6$ . The surface density of  $E < 18.8$ ,  $S_{1.4\text{GHz}} > 1$  mJy,  $z > 4$  QSOs is  $0.003 \text{ deg}^{-2}$ . This is currently the *only* well-defined sample of radio-loud QSOs at  $z \approx 4$  selected independently of radio spectral index. The QSOs are highly luminous in the optical (eight have  $M_B < -28$ ,  $q_0 = 0.5$ ,  $H_0 = 50 \text{ km s}^{-1} \text{ Mpc}^{-1}$ ). The SEDs are as varied as those seen in optical searches for high-redshift QSOs, but the fraction of objects with weak (strongly self-absorbed) Ly $\alpha$  emission is marginally higher (3 out of 18) than for high-redshift QSOs from SDSS (5 out of 96).

**Key words:** quasars: emission lines – quasars: general – early Universe – radio continuum: galaxies.

## 1 INTRODUCTION

The evolution with redshift of the space density of quasi-stellar objects (QSOs) places strong constraints on the abundance of massive objects at the earliest cosmological epochs. High-redshift QSOs can be found efficiently by colour selection from very large samples (e.g. the Sloan Digital Sky Survey, Anderson et al. 2001, see Benn et al. 2002, hereafter Paper I, for a summary of previous searches), but space-density measurements based on such selection could be biased by e.g. redshift-dependent dust extinction.

Any such bias is reduced when selecting in the radio, but searches for high-redshift radio QSOs have so far concentrated on radio-bright objects with flat radio spectra, which yield small samples with relatively low surface density on the sky. For example, Snellen et al. (2001) and Hook et al. (2002) sought red star-like optical counterparts of  $S_{5\text{GHz}} > 30$  mJy flat-spectrum radio sources, and identified a total of eight  $z > 4$  QSOs. Here, we aim to identify high-redshift radio quasars without any bias in radio spectral index, and with higher surface density on the sky, through spectroscopy of

red star-like counterparts of FIRST radio sources, with  $S_{1.4\text{GHz}} > 1$  mJy. Combined with our pilot search (Paper I), this yields 18  $z > 3.6$  radio-loud<sup>1</sup> QSOs (nine previously known, mainly from multicolour optical searches). This includes the largest sample to date of radio-selected QSOs at  $z > 4$ .

## 2 SAMPLE

The selection procedure is a refinement of that described in Paper I. We sought red, star-like optical identifications of the 722 354 sources in the 2000 July edition of the FIRST catalogue of radio sources [ $7988 \text{ deg}^2$ ,  $7^{\text{h}} < \text{RA} < 17^{\text{h}}$ ,  $-5^\circ < \text{Dec.} < 57^\circ$ , White et al. 1997,  $S_{1.4\text{GHz}}$  (peak)  $> 1$  mJy], satisfying the following criteria:

- (i) star-like optical counterpart in the Automated Plate Measurement facility (APM) (Irwin, McMahon & Maddox 1994) catalogue of the POSS-I survey (which includes  $7030 \text{ deg}^2$  of the FIRST survey), lying within 1.5 arcsec of the FIRST radio source;
- (ii) POSS-I/APM  $E < 18.8$ ;

<sup>1</sup> All 18 QSOs are radio-loud according to the criterion of Gregg et al. 1996, i.e.  $P_{1.4\text{GHz}} > 25.5$ ; see Table 1).

\*E-mail: j.holt@sheffield.ac.uk

**Table 1.** High-redshift radio QSOs in FIRST.

RA	Dec	$S_{1.4}$	$S_{4.85}$	$S_{10.6}$	$\alpha_{1.4-5}$	$\log_{10} L_R$	$R-O$	$E$	$O-E$	$R$	$I$	$z$	$\sigma_z$	$L_{\text{Ly}\alpha+\text{N V}}$	$D_A$	Notes
(J2000)	(2)	(3)	(4)	(5)	(6)	(7)	(8)	(9)	(10)	(11)	(12)	(13)	(14)	(15)	(16)	(17)
<i>z &gt; 3.6 QSOs with <math>O-E &gt; 3</math>, reported in this paper</i>																
09 18 24.38	06 36 53.5	26.5	38.5	23.1	0.30	27.09	0.2	18.7	> 3.0	19.5	18.6	4.180	0.010	<10	0.69	Véron-Cetty & Véron (2001), $z = 4.19$
10 13 47.31	06 50 15.6	31.0	14.1	6.2	-0.63	27.08	0.2	18.4	> 3.3			3.768	0.005	130	0.49	
10 53 20.42	-00 16 50.4	13.8	8.6	5.1	-0.38	26.82	0.8	18.1	> 3.6			4.289	0.005	120	0.61	Smith et al. (1994), $z = 4.291$
12 11 34.41	32 26 15.8	3.7	3.8		0.02	26.21	0.5	18.7	> 3.0	19.2	18.5	4.097	0.010	110	0.65	
13 03 48.96	00 20 10.3	1.1				25.59	0.2	18.7	> 3.0			3.638	0.005	40	0.55	Fan et al. (2000), $z = 3.655$
13 25 12.52	11 23 29.9	71.1	47.6	27.7	-0.32	27.55	0.6	18.8	> 2.9			4.400	0.010	140	0.64	Djorgovski et al. (2001), $z = 4.40$
14 00 12.06	17 20 01.3	15.2	14.9	8.1	-0.01	26.74	0.3	18.7	3.1			3.641	0.020	100	0.50	
14 12 05.80	-01 01 52.5	4.1	4.0		-0.01	26.19	0.5	18.8	> 2.9			3.720	0.010	50	0.51	Fan et al. (2000), $z = 3.73$
<i>z &gt; 3.6 QSOs with <math>O-E &gt; 3</math> reported by Benn et al. (2002)</i>																
07 25 18.29	37 05 17.9	26.6	28.2	16.1	0.05	27.11	0.6	18.3	> 3.4	19.5	18.7	4.330	0.010	80	0.69	
07 47 11.16	27 39 03.6	1.1				25.70	0.8	17.2	> 4.5			4.170	0.020	40	0.63	Richards et al. (2002)02, $z = 4.11$
08 31 41.68	52 45 17.1	1.3				25.72	0.7	15.3	3.9	14.5	13.9	3.870	0.030	<10	0.50	Irwin et al. (1998), $z = 3.91$
08 39 46.11	51 12 03.0	41.6	41.0	26.9	-0.01	27.32	0.8	18.5	> 3.2	18.9	18.3	4.420	0.020	110	0.54	Snellen et al. (2001), $z = 4.41$
09 41 19.36	51 19 32.3	2.5				26.00	1.3	17.6	> 4.1			3.850	0.010	25	0.58	
10 57 56.27	45 55 53.0	1.1				25.70	0.5	16.5	3.9	17.2	16.8	4.110	0.020	70	0.60	Stern et al. (2000), $z = 4.12$
12 20 27.93	26 19 03.6	35.0	6.0	2.4	-1.42	27.12	0.4	17.9	3.3			3.694	0.005	60	0.56	
13 09 40.61	57 33 09.1	11.3	7.5	3.7	-0.34	26.73	1.1	18.1	> 3.6	19.5		4.274	0.005	270	0.57	
14 23 08.19	22 41 57.5	35.4	24.2	4.6	-0.31	27.23	0.9	18.5	> 3.2	19.9	20.1	4.316	0.005	180	0.56	
16 39 50.51	43 40 03.3	25.2	15.9	9.8	-0.37	27.03	0.5	17.1	3.9	17.8	17.4	3.990	0.015	15	0.49	
<i>z &gt; 3 QSOs with <math>O-E &lt; 3</math> (i.e. not included in the sample of 121 candidates)</i>																
15 02 26.88	48 37 11.4	34.3				27.00	0.3	17.9	2.4			3.201	0.005	130	0.40	$O-E < 3$ , see Fig. 2
16 24 53.47	37 58 06.7	56.1				27.25	0.3	18.1	2.5			3.370	0.007	?	0.58	$O-E < 3$ , see Fig. 2

The columns give: (1, 2) optical right ascension and declination, (3) FIRST 1.4-GHz flux density (integrated, for  $S_{1.4\text{GHz}} > 10\text{ mJy}$ , otherwise peak), (4, 5) integrated Effelsberg 4.85- and 10.6-GHz flux densities, (6) radio spectral index  $\alpha$ ,  $S_\nu \propto \nu^\alpha$ , (7)  $\log_{10}$  radio luminosity ( $\text{W Hz}^{-1}$ ) (assuming  $H_0 = 50\text{ km s}^{-1}\text{ Mpc}^{-1}$ ,  $q_0 = 0.5$ , as used throughout in this paper, and assuming radio spectral index  $\alpha = -0.3$ , as used by Vigotti et al. 2003), (8) radio-optical position difference, (9, 10) APM POSS-I  $E$  magnitude and  $O-E$  colour, (11, 12) JKT  $R$ -band and  $I$ -band magnitudes, (13, 14) redshift and rms error on redshift, (15) approximate rest-frame Ly $\alpha$  equivalent width ( $\text{\AA}$ ),  $\pm 30$  per cent, (16) continuum decrement across Ly $\alpha$  line (Section 4.1.2), (17) notes. The first section of the table lists the 8  $z > 3.6$  QSOs discovered amongst the 60 spectra reported here. (Table 2 lists the remaining 52 candidates, and three with redshifts from the literature, and four candidates classified as galaxies on the basis of JKT imaging.) The second section of the table lists the 10  $z > 3.6$  QSOs discovered amongst the 54 spectra reported by Benn et al. (2002). The numbers 60, 3, 4 and 54 above sum to the total of 121 candidates. The third section reports two  $z > 3$  QSOs (with  $O-E < 3$ , not part of the sample) also discovered during the INT observations.

**Table 2.** Candidates which are not  $z > 3.6$  QSOs.

RA J2000 (1)	Dec J2000 (2)	$S_{1.4}$ mJy (3)	$R - O$ " (4)	$E$ (5)	$O - E$ (6)	ID (7)	$z$ (8)	$\sigma_z$ (9)	Notes (10)
Low-redshift QSOs and galaxies ('?' = probable galaxy)									
08 53 36.66	17 43 47.9	40.4	0.4	18.4	3.2	Q			Jaunsen et al. (1995), $z = 3.21$
09 29 00.44	16 28 06.3	4.8	0.9	17.0	>4.7	?			
09 41 39.71	35 32 33.5	4.6	0.6	18.8	>2.9	?			
09 44 28.41	06 41 44.7	3.2	0.8	18.6	>3.1	?			
10 01 42.41	20 48 18.2	2.2	0.5	18.6	>3.1	Q			Stoche et al. (1991), BL Lac, $z = 0.346$
10 08 34.99	35 51 23.4	6.5	1.1	18.6	>3.1	?			
10 13 08.38	08 27 15.7	28.5	0.4	18.7	>3.0	?			
10 24 42.51	56 11 25.1	0.8	0.3	18.7	>3.0	?			
10 25 06.45	19 15 44.6	2.0	0.7	18.6	>3.1	?			
11 34 58.18	12 32 21.2	6.7	0.5	18.0	3.3	?			
12 02 09.51	31 30 40.1	5.7	1.0	18.7	>3.0	?			
12 05 01.33	14 28 30.7	15.4	1.4	18.7	3.2	?			
12 20 16.87	11 26 28.2	2.3	0.4	18.1	3.6	Q	1.893	0.010	C III 1909, C III 2326, Mg II 2798 Å
12 39 32.76	-00 38 38.1	1.3	0.6	18.4	>3.3	Q			Boyle et al. (1990), BAL, $z = 2.18$
12 39 56.76	42 40 59.8	3.2	0.4	18.8	>2.9	?			
12 53 56.32	00 52 42.9	12.7	1.4	18.7	>3.0	?			
12 55 04.57	43 10 38.1	3.2	0.2	18.8	>2.9	?			
12 55 27.65	55 18 19.0	1.3	0.8	18.6	>3.1	?			
13 00 38.85	-03 35 16.8	1.4	0.6	17.4	3.1	G			Extended on JKT image, no spectrum obtained
13 00 53.46	-03 11 28.2	7.5	1.0	18.0	3.0	G			
13 06 21.99	03 36 06.3	2.0	0.8	18.4	>3.3	?			
13 10 43.44	43 39 04.8	4.7	0.7	18.6	>3.1	?			
13 18 51.57	-00 53 23.4	4.1	1.5	18.5	3.6	?			
13 32 29.08	26 34 33.2	1.3	0.3	18.8	>2.9	?			
13 39 43.42	40 34 25.4	1.0	1.0	18.7	>3.0	?			
13 43 14.20	22 08 45.7	1.5	0.4	18.4	>3.3	G			Extended on JKT image, no spectrum obtained
13 49 07.12	-02 23 24.9	3.1	0.4	18.0	>3.7	?			
14 13 59.17	02 55 27.2	1.1	0.3	17.9	3.1	G			
14 20 54.98	21 10 29.6	1.9	0.5	18.1	>3.6	G			
14 28 01.12	25 45 40.2	3.3	0.7	18.7	>3.0	?			
14 32 22.27	48 34 42.6	16.7	0.7	18.8	>2.9	S	0.1906	0.0005	O III 4959/5007, H $\alpha$
14 52 43.77	01 27 33.1	11.9	0.5	18.5	>3.2	?			
14 53 46.71	35 53 11.6	1.3	0.9	18.8	>3.0	G			
15 11 07.20	11 45 58.8	1.0	0.4	18.8	>2.9	G			Extended on JKT image, no spectrum obtained
15 34 22.24	18 51 25.2	1.5	0.3	18.4	3.2	?			
15 45 20.00	10 28 55.7	5.6	1.3	18.8	>3.0	G			
16 40 06.14	17 38 49.4	15.6	1.0	18.2	3.0	?			
17 00 01.29	19 29 31.6	2.7	0.8	18.7	>3.0	G			Extended on JKT image, no spectrum obtained
Stars									
09 01 46.15	15 02 21.8	3.7	1.3	18.6	>3.1	*			
09 09 53.20	03 01 35.8	1.5	0.5	18.6	>3.1	*			
09 12 20.95	14 18 48.3	1.8	1.5	18.4	>3.3	*			
09 17 33.46	08 56 30.7	2.1	1.4	17.9	3.7	*			
09 27 20.11	14 25 49.8	11.4	0.5	18.7	>3.0	*			
09 47 34.27	-01 51 31.7	7.5	0.8	18.4	3.2	*			
09 51 53.79	00 52 05.3	7.2	0.8	18.6	3.3	*			
11 07 19.77	15 16 20.1	14.3	1.2	18.0	3.0	*			
11 09 25.01	12 10 30.9	11.1	1.0	18.3	3.1	*			
11 22 09.69	02 13 36.8	2.3	1.2	17.9	>3.8	*			
12 13 06.97	13 43 07.3	62.7	0.5	18.4	3.1	*			
13 26 58.60	17 35 14.5	14.8	1.4	17.2	3.2	*			
14 33 23.85	37 39 08.9	15.8	1.2	18.7	>3.0	*			
14 49 00.23	07 37 36.2	1.3	1.3	18.5	>3.2	*			
15 14 50.17	06 36 05.3	2.4	1.2	17.2	3.3	*			
15 16 43.79	22 20 46.3	4.0	1.5	17.8	3.7	*			
15 39 59.30	-02 15 09.7	14.0	1.3	18.3	>3.4	*			
16 03 05.11	14 43 42.9	285.3	1.4	17.5	3.1	*			
16 23 57.72	23 50 12.0	2.5	1.0	18.8	>3.0	*			
16 41 53.13	12 55 12.7	1.8	0.6	17.8	3.4	*			
16 48 20.27	50 39 04.0	62.6	1.2	18.8	>2.9	*			

Columns 1–6 and 8–10 are as in Table 1. Column 7 indicates spectral type (see the caption of Fig. 3). For three of the QSOs, redshifts are available from the literature (indicated); spectra were not obtained for these.

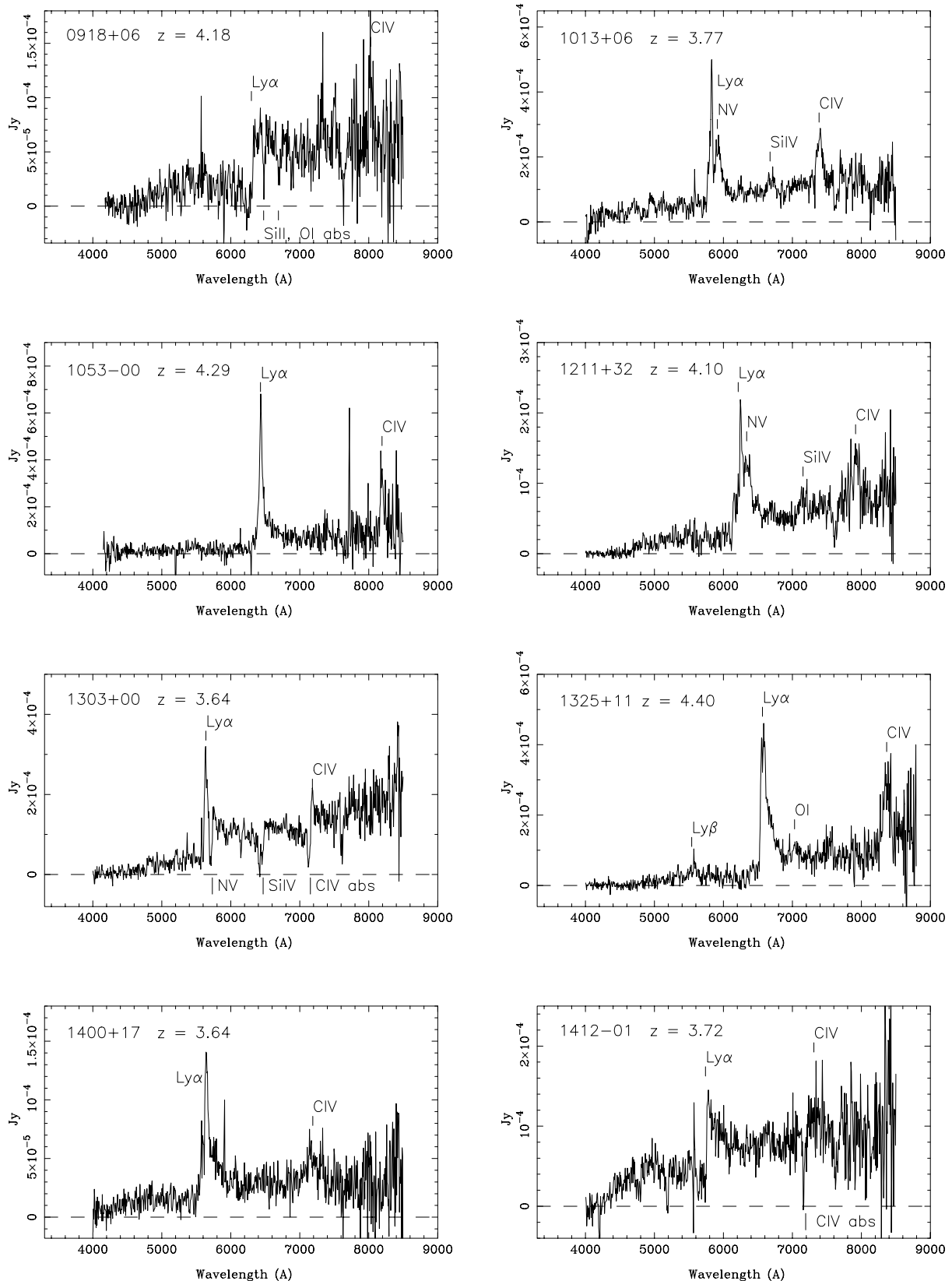


**Figure 1.** Spectra of the eight  $z > 3.6$  QSOs amongst the 60 newly observed candidates (see Paper I for those previously discovered). Spectral features are labelled at wavelengths corresponding to the quoted redshift, assuming rest-frame wavelengths in  $\text{\AA}$  of 1216 (Ly $\alpha$ ), 1240 (N v), 1302 (O I/Si II blend), 1400 (Si IV/O IV blend), 1549 (C IV). The spectra have not been corrected for terrestrial atmospheric absorption, notably at 7594 and 6867  $\text{\AA}$  (*A* and *B* bands). The ticks below the spectrum of 0918+06 indicate a  $z = 4.140$  absorption system (1260  $\text{\AA}$  Si II, 1302  $\text{\AA}$  O I/Si II, see also Snellen et al. 2001), i.e. velocity 2330  $\text{km s}^{-1}$  relative to the QSO. Those below the spectra of 1303+00 and 1412-01 indicate absorption at  $z = 3.600$  and  $3.624$ , respectively, i.e. outflow velocities 2600 and 6160  $\text{km s}^{-1}$ .

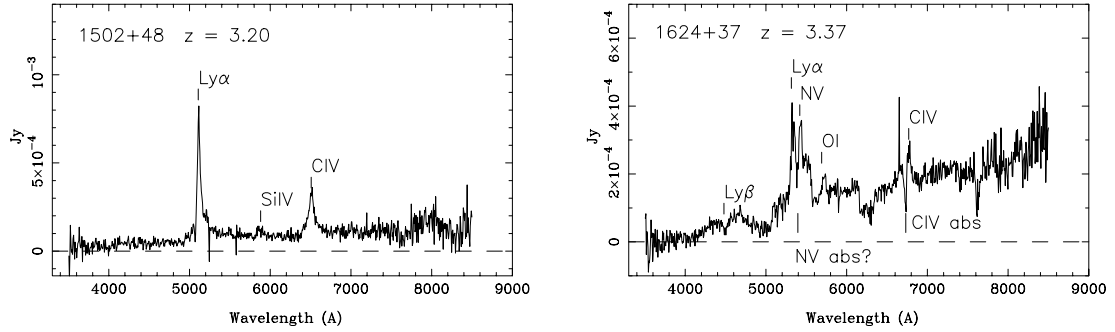


**Figure 2.** Spectra of two  $z > 3$  QSOs discovered when observing a sample of bluer,  $2.0 < O - E < 3.0$ , candidates (i.e. not included in the main sample of 121 observed candidates). The ticks below the spectrum of 1624+37 indicate an absorption system at  $z = 3.327$ , i.e. velocity  $2970 \text{ km s}^{-1}$  relative to the QSO. This QSO also exhibits a C IV broad absorption line, with outflow velocity up to  $29\,000 \text{ km s}^{-1}$ .

(iii) POSS-I/APM  $O - E \geq 3$ , or no measured  $O$  mag (plate limit  $O \approx 21.7$ );

(iv) star-like on POSS-II images (this excludes 80 per cent of candidates satisfying the above criteria);

(v) red also in the Minnesota APS (Pennington et al. 1993) catalogue of the POSS-I plates, i.e. not omitted from the APM catalogue because of confusion on the blue plate, see Paper I (this excludes 16 per cent of the candidates satisfying the above criteria).

This yielded 294 candidates, of which we visually classified 194 as ‘star-like’ on POSS-II and 100 as ‘possibly star-like’.

CCD images were obtained in good seeing of approximately one-third of these, using the Loiano 1.5-m telescope of the Astronomical Observatory of Bologna. On these images, 25 of the 70 ‘star-like’ on POSS-II and 28 of the 33 ‘possibly star-like’ candidates were extended. We therefore excluded from our sample the 100 ‘possibly star-like’ objects, implying an incompleteness of  $100 \times 5/33 = 15.2$  stellar candidates.

The final list of 194 candidates is therefore expected to include  $45/70 \times 194 = 124.7$  truly star-like images, out of a total of  $124.7 + 15.2 = 139.9$  amongst the original list of 294 candidates. Therefore, it includes 89 per cent ( $= 124.7/139.9$ ) of the red QSO identifications of sources in this edition of the FIRST catalogue. The selection criteria differ from the preliminary criteria used in Paper I only in going slightly deeper, i.e.  $E < 18.8$  rather than  $E < 18.6$ .

### 3 OBSERVATIONS AND REDUCTION

#### 3.1 Optical spectroscopy

Observations of 54 of the 194 candidates were reported in Paper I. The 55th object reported there, 1349+38, is actually detected on the Minnesota APS scan of the POSS-I blue plate (i.e. it is not red), and thus does not meet selection criterion (v) above. Spectra were obtained of 60 more candidates using the IDS spectrograph on the Isaac Newton Telescope during near-photometric nights (occasional light cirrus) in 2001 May. The spectrograph was used with the R150V grating, yielding spectra with dispersion  $6.5 \text{ \AA pixel}^{-1}$ , usually centred at  $6500 \text{ \AA}$ . For details of the observing and data-reduction, refer to Paper I. The results are summarized in Tables 1 ( $z > 3.6$  QSOs) and 2 (other objects). Table 2 includes an additional three QSOs, which were not observed, but where the redshifts were obtained from the literature. Spectra of the QSOs with redshift  $z > 3.6$  are shown in Fig. 1.

To test the completeness of the search for  $z > 4$  QSOs, we observed an additional 28 candidates with  $2.0 < O - E < 3.0$ . None

had  $z > 3.6$ . The spectra of two objects with  $z = 3.2, 3.4$  are given in Fig. 2 (details included in Table 1).

In total, we have spectroscopic information for 117 of the 194 candidates with  $O - E > 3$  (54 observed Paper I, 60 observed here, three redshifts  $z < 3.6$  from the literature). In addition, we were able to classify four objects as galaxies on the basis of Jacobus Kapteyn Telescope (JKT) imaging (see below). The colour–magnitude distribution of these 121 candidates is shown in Fig. 3.

The distribution of our 18  $z > 3.6$  QSOs in radio flux density and  $E$  mag is compared with that from other radio searches for high-redshift QSOs in Fig. 4. In the optical, these QSOs are highly luminous, most with  $M_{\text{AB}}(1450 \text{ \AA}) < -27$ .

Of the 121 observed candidates, 18 (15 per cent) are QSOs with  $z > 3.6$  and 10 of these have  $z > 4$ .

#### 3.2 Optical imaging

Some of the 194 candidates were imaged through a Harris  $R$  filter with the 1.0-m Jacobus Kapteyn Telescope in service time, in order to identify extended objects. Spectra were later obtained of most of these candidates at the INT (above), but the ‘G’ (galaxy) classifications of four objects in Table 2 are based on JKT imaging alone.

In addition, Harris  $R$ - and  $I$ -band photometry was obtained with the JKT (see Table 1) for nine of the  $z > 3.6$  QSOs, primarily to allow an independent check of the derivation of  $M_{\text{AB}}(1450 \text{ \AA})$  absolute magnitudes (see Vigotti et al. 2003). Conditions were photometric, except for light cirrus during observation of 1639+43. Otherwise, the estimated errors on the  $R, I$  mag are  $< 0.05$  mag. For smooth continuum spectra, one would expect POSS-I  $E$  and JKT  $R$  mag to differ by  $< 0.1$  mag (Humphreys et al. 1991), at a given epoch. The observed  $R - E$  values range from  $-0.8$  to  $1.4$  (median 0.7), mainly because the  $R$  filter covers a wavelength range a factor of three larger than does the  $E$  filter, and includes more of the depressed continuum blueward of  $\text{Ly}\alpha$ . The range of  $R - E$  values may also reflect changes in QSO luminosity during the 50 yr between the POSS-I and JKT observations.

#### 3.3 Radio observations

The 13  $z > 3.6$  QSOs with  $S_{1.4 \text{ GHz}} > 3 \text{ mJy}$  were observed at 4.85 and 10 GHz, with the Effelsberg radio telescope, during the night of 2002 January 13. The sources are all unresolved by the telescope beam, FWHM 143 and 69 arcsec at these two frequencies. The sources were observed by scanning the telescope in right ascension and

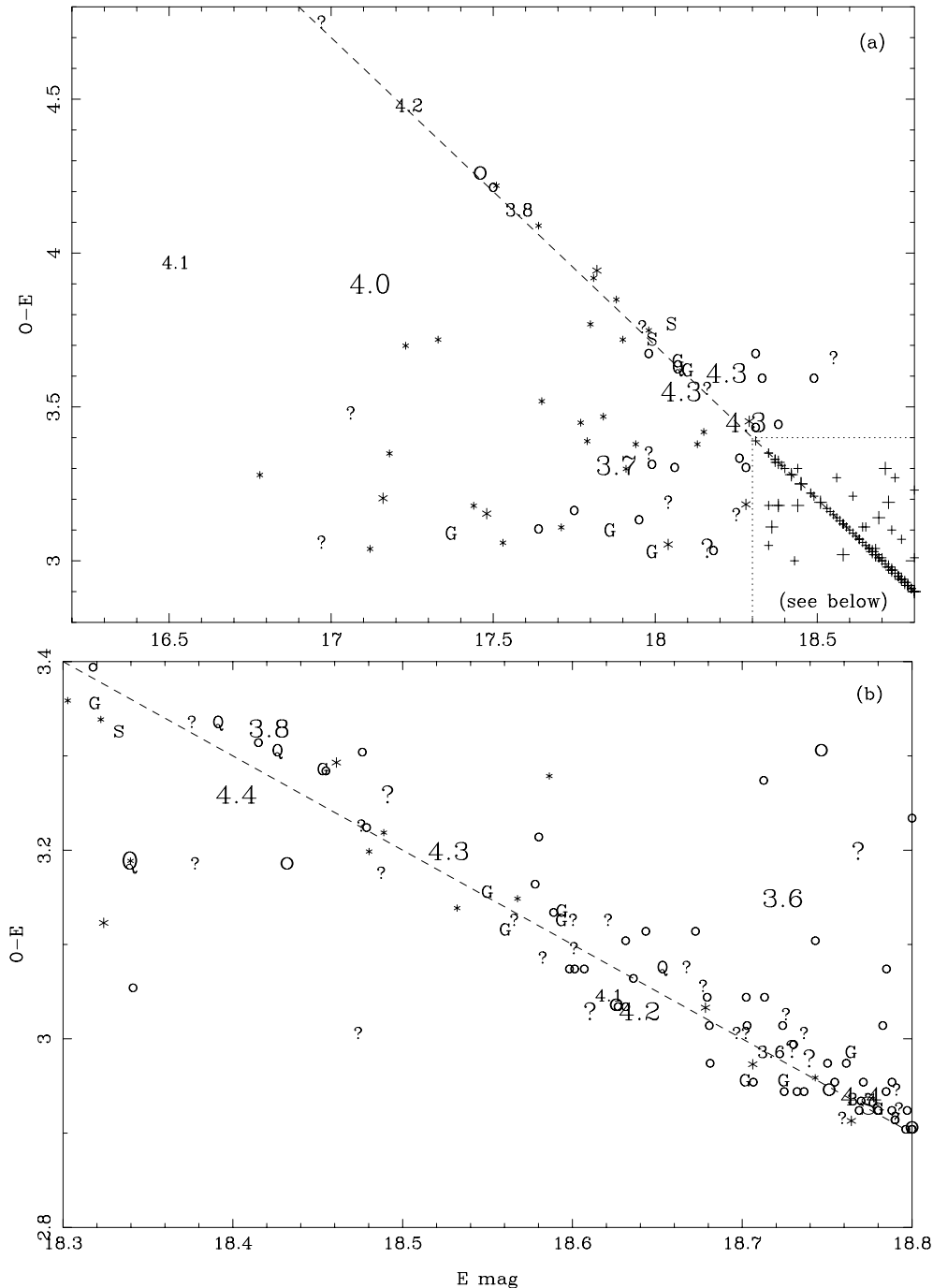


**Figure 3.** (a) Distribution in colour and magnitude of the 194 star-like candidates. (b) Expanded view of the lower-right-hand corner of Fig. 3(a). The symbols for spectral type (121 objects) are: number = redshift of QSO with  $z > 3.6$ , ‘Q’ = QSO with  $z < 3.6$ , ‘S’ = emission-line galaxy (starburst or Seyfert), ‘G’ = radio galaxy, ‘?’ = probable radio galaxy (definitely not high-redshift QSO, but might be a star), ‘\*’ = star. Large font indicates  $S_{1.4\text{GHz}} > 10$  mJy; small font  $S_{1.4\text{GHz}} < 10$  mJy. Objects with no  $O$  magnitude have been plotted at the nominal  $O$  plate limit (dashed line) with  $O - E = 21.7 - E$ . The unobserved 73 = 194 - 121 objects are plotted as circles. In Fig. 3(a), the positions of a few points have been adjusted to reduce overlap of labels. In Fig. 3(b), the  $E$  mag have been randomized  $\pm 0.05$  mag for the same reason.

declination, with scan speeds 30 and 10 arcmin  $\text{min}^{-1}$  respectively, scan lengths 15 and 7 arcmin, with the total number of scans adjusted to the total flux density of each source. The flux densities (scale of Baars et al. 1977) and spectral indices (between 1.4 and 4.85 GHz) are given in Table 1. The median spectral index is  $\alpha = -0.3$  ( $S_\nu \propto \nu^\alpha$ ).

## 4 RESULTS

### 4.1 High-redshift QSOs

The sample comprises 18  $z > 3.6$  QSOs (Table 1). Below we derive the surface density on the sky, and we comment on the spectra of individual objects.

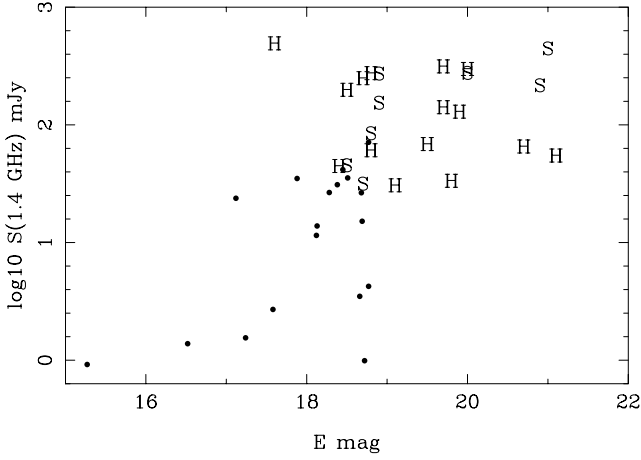


**Figure 4.** Distribution in  $S_{1.4\text{GHz}}$  and  $E$  mag of  $z > 3.6$  radio-selected QSOs. ● = FIRST QSOs (Table 1), S = Snellen et al. (2001), H = Hook et al. (2002). See also Isaak et al. (2002) for a list of 17  $z > 4$  optically- and X-ray-selected QSOs with known radio counterparts.

#### 4.1.1 Surface density

The fraction of high-redshift QSOs amongst the candidates does not depend on optical magnitude, but depends strongly on radio flux density (Table 3): 8 per cent for  $S_{1.4\text{GHz}} < 10$  mJy, 37 per cent for  $S_{1.4\text{GHz}} > 10$  mJy. 73 of the 194 candidates have not been observed, 67 with  $S_{1.4\text{GHz}} < 10$  mJy, 6 with  $S_{1.4\text{GHz}} > 10$  mJy. On the basis of the above high-redshift-QSO fractions, we expect to have missed 5.95  $z > 3.6$  QSOs in the sample of 194 candidates, i.e. the completeness of our search for candidates satisfying our selection criteria is  $[18/(18 + 5.95)] = 75$  per cent over the  $7030 \text{ deg}^2$  overlap between FIRST and the APM/POSS-I catalogues, within  $7^{\text{h}} < \text{RA} < 17^{\text{h}}$ . Multiplying by the 89 per cent completeness due to filtering out ‘possibly star-like’ candidates (Section 2), our search is 67 per cent complete, i.e. the surface density of  $z > 4$  QSOs (10 QSOs  $E < 18.8$ ,  $S_{1.4\text{GHz}} > 1$  mJy) found with this technique is  $0.0021 \text{ deg}^{-2}$ .

This is approximately twice that of recent searches for high-redshift QSOs amongst the red star-like optical counterparts of (radio-brighter) flat-spectrum sources in the northern (Snellen et al. 2001; four  $z > 4$ ,  $E < 19$ ,  $0.0006 \text{ deg}^{-2}$ ) and southern (Hook et al. 2002; four  $z > 4$ ,  $S_{5\text{GHz}} > 72$  mJy,  $R < 22.5$ ,  $0.001 \text{ deg}^{-2}$ ) hemispheres. The surface densities measured for the FIRST sources are higher in part because of the much fainter radio flux-density limit, and in part because steep-spectrum sources are not excluded.

In the sample of Hook et al. (2002), the ratio of the numbers of  $E < 21$  and  $E < 19$   $z > 4$  QSOs is  $7/4 = 1.8$ . Combining this with

our above result, we predict the surface density of  $E < 21$ ,  $S_{1.4\text{GHz}} > 1$  mJy QSOs with  $z > 4$  to be  $0.004 \text{ QSOs deg}^{-2}$ .

The surface-density calculations above account for incompleteness due to rejection of candidates not considered definitely star-like on POSS-II, and due to only 121 out of 194 candidates being observed. In calculating the overall completeness of a search for  $z > 4$  QSOs with  $S_{1.4\text{GHz}} > 1$  mJy, one must also take into account:

- (i) the completeness of the FIRST catalogue at low flux densities, 83 per cent for the flux-density distribution of Table 1 (Prandoni et al. 2001);
- (ii) the completeness of the APM catalogue of POSS-I, 84 per cent (see Vigotti et al. 2003, Section 2.3);
- (iii) that the radio-optical separations of some QSOs may exceed 1.5 arcsec, due to measurement errors, completeness 99 per cent, given combined radio-optical rms 0.5 arcsec;
- (iv) that some QSOs may be missed because they do not coincide with peaks of radio emission (e.g. near the mid-points of double radio sources), completeness 98 per cent (see Vigotti et al. 2003, Section 2.3);
- (v) that some  $z > 4$  QSOs may have  $O - E < 3$ , completeness  $\sim 100$  per cent (Section 3.1, see also Vigotti et al. 2003, fig. 1).

The completeness due to these five factors combined is 0.68, i.e. the corrected surface densities of  $z > 4$  QSOs with  $S_{1.4\text{GHz}} > 1$  mJy is  $0.0031 \text{ deg}^{-2}$  for  $E < 18.8$  and is  $0.006 \text{ deg}^{-2}$  for  $E < 21$ .

Since  $\sim 10$  per cent of QSOs are radio-loud (e.g. Sramek & Weedman 1980; and Petric et al. 2003 for consistency at  $z \sim 5$ ), we expect the density of radio-quiet + radio loud  $z > 4$  QSOs with  $E < 21$  to be  $\sim 0.06 \text{ deg}^{-2}$ . E.g. Kenefick et al. (1995a); Kenefick, Djorgovski & de Carvalho (1995b) find  $0.03 \text{ deg}^{-2}$  with  $r < 20$ . The SDSS search (e.g. Anderson et al. 2001) reaches a higher surface density,  $\sim 0.1 \text{ deg}^{-2}$  because the  $i$  and  $z$  bands are also used, i.e. no effective limit in  $r$  band.

#### 4.1.2 Ly $\alpha$ emission

The rest-frame Ly $\alpha$  + N v equivalent widths of the 18  $z > 3.6$  QSOs are given in Table 1. The values are approximate, rms  $\sim 30$  per cent, due to the difficulty of estimating the slope of the underlying continuum (see e.g. Schneider, Schmidt & Gunn 1991), but the median value of  $75 \text{ \AA}$  is similar to that reported elsewhere for  $z \sim 4$  QSOs,  $\sim 70 \text{ \AA}$  (Fan et al. 2001; Constantin et al. 2002). However, three of our 18 radio-selected QSOs have rest-frame equivalent widths  $< 25 \text{ \AA}$ : 0831+52 ( $< 10 \text{ \AA}$ ), 0918+06 ( $< 10 \text{ \AA}$ ) and 1639+40 ( $\sim 15 \text{ \AA}$ ), presumably because the lines are heavily self-absorbed. By comparison, only 5 out of 93 optically selected SDSS QSOs  $z > 3.6$  (from Fan et al. 1999a, 2000, 2001; Anderson et al. 2001; Schneider et al. 2001) exhibit such small Ly $\alpha$  equivalent

**Table 3.** Fractions of candidates which are QSOs with  $z > 3.6$ .

$S_{1.4\text{GHz}}$ (1)	$E < 17.8$ (2)	$17.8 < E < 18.3$ (3)	$E > 18.3$ (4)	All (5)	All per cent (6)
$< 3$	4/16	0/13	1/28	5/57	9
3–10	0/7	0/8	2/19	2/34	6
$> 10$	1/3	4/9	6/18	11/30	37
All	5/26	4/30	9/65	18/121	15
All per cent	19	13	14	15	

Columns are: (1) FIRST 1.4-GHz integrated flux density (mJy), (2–4) number of  $z > 3.6$  QSOs/total number of candidates, for each range of POSS-I  $E$  magnitude, (5) sum over all ranges of  $E$  and (6) sum expressed as a percentage.

widths (but see Fan et al. 1999b for an example of a  $z = 4.62$  QSO with no emission lines at all). The difference between the two samples is weakly significant. Our sample of QSOs and that from SDSS have similar median redshift, so the difference cannot be ascribed to a difference in epoch (e.g. at  $z > 5.7$ , Fan et al. 2003 found that 1 out of 3 QSOs has  $\text{Ly}\alpha$  equivalent width  $\leq 25 \text{ \AA}$ ). A difference might also arise due to the inverse correlation between emission-line equivalent width and optical luminosity known at low redshift, the Baldwin effect (Baldwin, Wampler & Gaskell 1989). The optical luminosities of our QSOs are indeed  $\sim 2$  mag higher than those from SDSS, but Constantin et al. (2002) found the Baldwin effect to be weak or absent for QSOs with  $z > 4$ . Finally, the difference might be connected with the fact that our QSOs host a radio source, although previous studies (e.g. Corbin 1992) have found that emission-line strengths do not depend on whether a QSO is radio loud or quiet. If one combines our radio-selected sample (18 QSOs) with the radio-selected (but radio brighter) samples of Hook et al. (2002; 13 QSOs  $z > 3.6$  with spectra) and of Snellen et al. (2001; four QSOs  $z > 3.6$ , one already included in our sample), the fraction with  $\text{Ly}\alpha$  equivalent widths  $< 25 \text{ \AA}$  reduces to 3 out of 34, i.e. not significantly different from SDSS.

High-redshift QSOs are also characterized by a drop in the continuum across the  $\text{Ly}\alpha$  line, from red to blue, due to absorption by neutral hydrogen along the line of sight. The measured values of the opacity  $D_A = (1 - f_1/f_2)$ , where  $f_1$  and  $f_2$  are the intensities in the continuum regions 1050–1170 and 1250–1350  $\text{\AA}$ , respectively, (Oke & Korycansky 1982), are given in column 16 of Table 1. The error in measured  $D_A$  is  $\sim 10$  per cent. The median  $D_A$  for the eight QSOs with  $3.6 < z < 4.0$  is 0.50, while that for the 10 QSOs with  $4.0 < z < 4.4$  is 0.62, consistent with the trend with redshift observed by (their fig. 5 Kennefick et al. (1995b, their fig. 5) for optically selected QSOs.

#### 4.1.3 Narrow absorption lines

The QSOs 0831+52, 0918+06, 0941+51, 1303+00 and 1412-01 show metal-line absorption features at velocities relative to the QSO ranging 1200 to 7000  $\text{km s}^{-1}$ . QSOs 0831+41, 0918+06, 0941+51 and 1303+00 exhibit absorption at velocity separations below 3000  $\text{km s}^{-1}$  (i.e. probably associated with the QSO). 0831+41 and 1412-01 exhibit absorption systems at higher velocities. Metal absorption lines are not visible in our spectrum of 0747+27, but in a high-resolution spectrum obtained by Richards et al. (2002), at least 14 independent C IV absorption systems are detected.

#### 4.1.4 BAL QSOs

One of the 18  $z > 3.6$  QSOs, 0831+41, is classified as a broad-absorption-line (BAL) QSO by Irwin et al. (1998). Fan et al. (2001) found two classical BALs in their sample of 39 high- $z$  QSOs. The BAL fraction in both our sample and that of Fan et al. is consistent with the fraction 10 per cent found for low-redshift optically selected QSOs (Weymann et al. 1991).

1624+37 ( $z = 3.4$ , i.e. not included in the sample of 18  $z > 3.6$  QSOs, see Table 1) is a new BAL QSO. The C IV absorption feature has FWHM  $\sim 9000 \text{ km s}^{-1}$  and is detached by 20 000  $\text{km s}^{-1}$  from the peak of the emission. It has an unusually sharp high-velocity cut-off.

## 4.2 Low-redshift objects

The remaining candidates (Table 2) are a mixture of low-redshift QSOs, emission-line galaxies, absorption-line galaxies and stars. The QSOs and galaxies are mostly true identifications, the stars

are mostly misidentifications, as is implied by the distributions of radio-optical separations in Table 2 (although the higher values for stars might also be attributed to proper motion between the epochs of POSS-I and the FIRST survey). The distribution of radio flux-densities of the sources apparently identified with stars is statistically indistinguishable from that of the FIRST catalogue as a whole. We obtained deep images at the JKT,  $R < 24$ , of two M stars lying close to  $S_{1.4\text{GHz}} \sim 100 \text{ mJy}$  sources (0741+33,  $E = 18.4$  and 1353+34,  $E = 17.8$  from Paper I), but a host galaxy is not detected in either case, so we cannot reject the hypothesis that these are true radio stars.

A ‘?’ classification in Table 2 indicates that there was insufficient signal-to-noise ratio to distinguish between galaxy and M-star spectra, but that the spectrum is not consistent with that of a  $z \sim 4$  QSO (i.e. we expect there to be  $\lesssim 1$  such QSO hidden amongst the ‘?’ objects).

## 5 CONCLUSIONS

We identified 194 high-redshift QSO candidates that:

- (i) coincide with FIRST radio sources  $S_{1.4\text{GHz}} > 1 \text{ mJy}$ ;
- (ii) are classified star-like on APM (POSS-I) and on POSS-II;
- (iii) have APM  $E < 18.8$  and  $O - E \geq 3.0$ , or are invisible on the  $O$  plate.

The sample covers an area of 7030  $\text{deg}^2$ . We have observed 121 of the candidates and find 18 to be QSOs with  $z > 3.6$ , 10 of these with  $z > 4$  (Paper I and this paper). We estimate that we have found 75 per cent of the high-redshift QSOs present amongst the 194 candidates. The surface density of  $z > 4$  QSOs with  $E < 18.8$ ,  $S_{1.4\text{GHz}} > 1 \text{ mJy}$ , is  $0.0031 \text{ deg}^{-2}$ .

This is currently the *only* well-defined sample of  $z \approx 4$  radio QSOs selected independently of radio spectral index. Vigotti et al. (2003) use a subsample of 13 of these QSOs, with  $z > 3.8$ ,  $M_{\text{AB}}(1450 \text{ \AA}) > -26.9$  and  $\log P_{1.4\text{GHz}}(\text{W Hz}^{-1}) > 25.7$ , to measure the space density of QSOs at  $z = 4$  and determine the change in space density between  $z = 2$  and 4.

These QSOs are highly luminous in the optical (eight have  $M_B < -28$ ,  $q_0 = 0.5$ ,  $H_0 = 50 \text{ km s}^{-1} \text{ Mpc}^{-1}$ ). The SEDs are remarkably varied. They include: three QSOs with very weak  $\text{Ly}\alpha$  (0831+52, 0918+06, 1639+40), one with an unusually high density of C IV absorption systems (0747+27, Richards et al. 2002), one with a probable DLA (0941+51), the luminous and much-studied 0831+52 (Irwin et al. 1998) and a QSO with narrow  $\text{Ly}\alpha$  of high equivalent width (1309+57). 1624+37 (outside the sample) is an unusual BAL QSO.

## ACKNOWLEDGMENTS

JH was a 1-yr placement student at ING during 2000–2001. RC and JIGS acknowledge financial support from DGES project PB98-0409-C02-02. CRB, MV, RC and JIGS acknowledge financial support from the Spanish Ministerio de Ciencia y Tecnologia under project AYA2002-03326. KHM was supported through a European Community Marie Curie fellowship. The Isaac Newton and the Jacobus Kapteyn Telescopes are operated on the island of La Palma by the Isaac Newton Group in the Spanish Observatorio del Roque de los Muchachos of the Instituto de Astrofísica de Canarias. The 100-m Effelsberg radio telescope is operated by the Max-Planck-Institut für Radioastronomie. The APS Catalog of POSS-I (<http://aps.umn.edu>) is supported by NASA and the University of Minnesota. We are grateful to the anonymous referee for helpful suggestions.



## REFERENCES

- Anderson S.F. et al., 2001, *AJ*, 122, 503
- Baars J.W.M., Genzel R., Pauliny-Toth I.I.K., Witzel A., 1977, *A&A*, 61, 99
- Baldwin J.A., Wampler E. J., Gaskell C. M., 1989, *ApJ*, 338, 630
- Benn C.R., Vigotti M., Pedani M., Holt J., Mack K.-H., Curran R., Sánchez S.F., 2002, *MNRAS*, 329, 221 (Paper I)
- Boyle B.J., Fong R., Shanks T., Peterson B.A., 1990, *MNRAS*, 243, 1
- Constantin A., Shields J.C., Hamann F., Foltz C., Chaffee F.H., 2002, *ApJ*, 565, 50
- Corbin M., 1992, *ApJ*, 391, 577
- Djorgovski S.G., 2001, <http://astro.caltech.edu/~george/z4.qsos>
- Fan X. et al., 1999a, *AJ*, 118, 1
- Fan X. et al., 1999b, *ApJ*, 526, L57
- Fan X. et al., 2000, *AJ*, 119, 1
- Fan X. et al., 2001, *AJ*, 121, 31
- Fan X. et al., 2003, *AJ*, 125, 1649
- Gregg M.D., Becker R.H., White R.L., Helfand D.J., McMahon R.G., Hook I.M., 1996, *AJ*, 112, 407
- Hook I.M., McMahon R.G., Shaver P.A., Snellen I.A.G., 2002, *A&A*, 391, 509
- Humphreys R.M., Landau R., Ghigo F.D., Zumach W., Labonte A.E., 1991, *AJ*, 102, 395
- Irwin M.J., McMahon R.G., Maddox S., 1994, *Spectrum* no. 2, p. 14
- Irwin M.J., Ibata G.F., Lewis G.F., Totten E.J., 1998, *ApJ*, 505, 529
- Isaak K.G., Priddey R.S., McMahon R.G., Omont A., Peroux C., Sharp R.G., Withington S., 2002, *MNRAS*, 329, 149
- Jaunsen A.O., Jablonski M., Pettersen B.R., Stabell O., 1995, *A&A*, 300, 323
- Kennefick J.D., de Carvalho R.R., Djorgovski S.G., Wilber M.M., Dickson E.S., Weir N., Fayyad U., Roden J., 1995a, *AJ*, 110, 78
- Kennefick J.D., Djorgovski S.G., de Carvalho R.R., 1995b, *AJ*, 110, 2553
- Oke J.B., Korycansky D.G., 1982, *ApJ*, 255, 11
- Pennington R.L., Humphreys R.M., Odewahn S.C., Zumach W., Thurmes P.M., 1993, *PASP*, 105, 521
- Petric A.O., Carilli C.L., Bertoldi F., Fan X., Cox P., Strauss M.A., Omont A., Schneider D.P., 2003, *AJ*, 126, 15
- Prandoni I., Gregorini L., Parma P., de Ruiter H. R., Vettolani G., Wieringa M. H., Eleers R. D., 2001, *A&A*, 365, 392
- Richards G.T., Gregg M.D., Becker R.H., White R.L., 2002, *ApJ*, 567, L13
- Schneider D.P., Schmidt M., Gunn J. E., 1991, *AJ*, 101, 2004
- Schneider D.P. et al., 2001, *AJ*, 121, 1232
- Smith J.D., Thompson D., Djorgovski S., 1994, *AJ*, 107, 24
- Snellen I.A.G., McMahon R.G., Dennett-Thorpe J., Jackson N., Mack K.-H., Xanthopoulos E., 2001, *MNRAS*, 325, 1167
- Sramek R.A., Weedman D.W., 1980, *ApJ*, 238, 435
- Stern D., Djorgovski S.G., Perley R.A., de Carvalho R.R., Wall J.V., 2000, *AJ*, 119, 1526
- Stocke J.T., Morris S.L., Gioia I.M., Maccacaro T., Schild R., Wolter A., Fleming T.A., Henry J.P., 1991, *ApJS*, 76, 813
- Véron-Cetty M.-P., Véron P., 2001, *A&A*, 374, 92
- Vigotti M., Carballo R., Benn C.R., de Zotti G., Fanti R., González-Serrano J.I., Mack K.-H., Holt J., 2003, *ApJ*, 591, 43
- Weymann R.J., Morris S.L., Foltz C.B., Hewett P.C., 1991, *ApJ*, 373, 2
- White R.L., Becker R.H., Helfand D.J., Gregg M.D., 1997, *ApJ*, 475, 479

This paper has been typeset from a  $\text{\TeX}/\text{\LaTeX}$  file prepared by the author.